Magazine of Civil Engineering

ISSN 2712-8172

journal homepage: http://engstroy.spbstu.ru/

DOI: 10.34910/MCE.104.12

Ultimate load capacity of high-performance fibre-concrete hollow square columns

***K. Buka-Vaivade*[a], *D. Serdjuks**[a], *J. Sliseris*[a], *L. Pakrastins*[a], *N. Vatin*[b]**

[a] *Riga Technical University, Riga, Latvia*

[b] *Peter the Great St. Petersburg Polytechnic University, St. Petersburg, Russia*

**E-mail: Dmitrijs.Serdjuks@rtu.lv*

Keywords: high-performance fibre-reinforced concrete, hollow square section, hollow concrete column, finite element method, response surface method, eccentric loading, computational time reduction, simplified analytical calculation

Abstract. High-performance fibre-reinforced concrete is gaining popularity due to fibres ability to improve the poor properties of high-performance concrete. High-performance materials make using of thin-wall structures possible. Square section with square hollow provides decreasing of non-renewable material consumption, column's high stiffness in the both planes and possibility to integrate the engineering communication inside of columns. The current study focuses on the development of analytical simplified calculation method that approximate output results of finite elements calculations for columns under eccentric loading with complicate hollow square-section. Analytical simplified calculation method to determine column's load-carrying capacity is developed as the second-degree polynomial equation which is based on response surface method. The variables of equation are column height and material consumptions of the high-performance fibre reinforced concrete and steel of the additional longitudinal reinforcement. Data set of 27 experiments calculations was used to get the coefficients of adequate equation. Based on the results, the obtained equation makes it possible to predict the load-carrying capacity of the column in selected the factors interval on which a function was defined with sufficient precision. The difference between load-carrying capacities determine by numerical model based on the finite element method and by obtained second-degree equation does not exceeds 3.3 %.

1. Introduction

The object of this investigation is determination of ultimate load capacity of hollow high-performance steel fibre reinforced concrete column with height 3.5–4.5 m and variable consumptions of concrete and steel of additional longitudinal reinforcement.

As total world population continues to grow rapidly, the principle of sustainable development is becoming ever more important. Therefore, the problem of how to make the best use of limited non-renewable resources to satisfy unlimited human wants is actual now. Concrete is the most used man-made construction material. High-performance concrete is characterized by higher specific strengths than ordinary concrete, so its use in load-bearing structures is more rational. Fibres can be used to decrease fragility of the high-performance concrete and to improve the deformative properties of the concrete [1–14]. High-performance steel fibre reinforced concrete allows constructive solutions like thin-wall structures, which reduce material consumption and dead load of structures.

The interest of the use of hollow concrete columns is growing due to several reasons, including their effective section properties in terms of higher strength/mass and stiffness/mass ratios compared to solid sections with the same cross-section area; reduced weight of the structure and, accordingly, the overall foundation sizes, therefore also reduced cost and environmental impact; provided space to integrate the engineering communications inside of columns and to allow access for services of plumbing and electric wiring [15–21]. In addition to these benefits, as investigations of hollow concrete columns behaviour show,

Buka-Vaivade, K., Serdjuks, D., Sliseris, J., Pakrastins, L., Vatin, N. Ultimate load capacity of high-performance fibre-concrete hollow square columns. Magazine of Civil Engineering. 2021. 104(4). Article No. 10412. DOI: 10.34910/MCE.104.12

the capacity of hollow concrete columns is comparable to solid columns or even higher, because of difference in the stress distributions in the column sections. The absence of the concrete core changes triaxial stress state as it is in solid concrete columns to biaxial stress distribution in hollow concrete columns sections [19]. One of the most important problem of the hollow concrete columns is low deformation capacity resulting in brittle failure behaviour [18–19]. The use of discrete fibres is recognized as a successful solution to this problem [17, 21].

There are many studies [22–26] that confirm high computational cost of high-performance fibre reinforced concrete structural analyses based on finite element models. Calculations with the 3D numerical model with huge number of finite elements are complex and time-consuming, therefore the options of using finite element models with larger element sizes [22], symmetrical conditions [23–25] and two or one-dimensional numerical models [26–27] are generally selected to achieve reliable results with less computational time. So, the aim of this investigation is to develop simplified analytical calculation method that approximate ultimate load capacity output results of finite elements calculations for hollow high-performance steel fibre reinforced concrete column under eccentric loading. Proposed method is based on response surface methodology. Several tasks of the study have been set for this purpose. The first task is validation of the 3D numerical model by experimental data to determine accuracy of finite element model of high-performance fibre reinforced concrete structure. The second task is comparison of calculation results obtained by 3D numerical model and 1D numerical model, to evaluate possibility of reducing of computational time by using simplified 1D numerical model. And the last task is experimental design to get experimental data set for development of the second order polynomial equation on which the method to be developed is based. The field of application of the simplified analytical calculation method, which makes it possible to predict the results of the ultimate load capacity of the hollow high-performance fibre reinforced concrete column in selected region of interest is the initial design stage, during which it is necessary to determine the used structures approximate dimensions and materials.

2. Methods

2.1. Object of investigation

A hollow square-section column (Fig. 1) subjected to the compression and bending was considered as an object of this investigation. Constant 500×500 mm external dimensions and variable hollow square-section wall thickness t was taken. As a basis of the high-performance steel fibre reinforced concrete material high-performance concrete of class C60 /75 [28] with 1 % of steel RC 65/35 BN-type fibres are used. Composition of used material is taken from the publication [29]. Steel of class B550 is used for additional longitudinal reinforcement of the column.

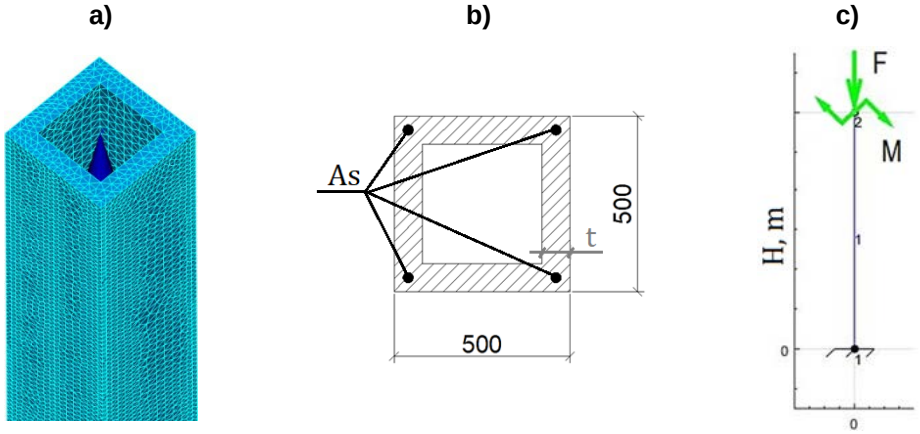

Figure 1. Details of column structure: a) column 3D numerical model with meshing; b) hollow square-section of column with longitudinal reinforcement; c) design scheme of the column.

As the factors interval on which a function was defined for the column subjected to the compression and flexure variable parameters for analytical simplified calculation method to determine column ultimate load capacity are chosen column height H from 3.5 to 4.5 m and material consumption of the high-performance fibre reinforced concrete and steel of the additional longitudinal reinforcement by regulation of variable from 5 to 12 cm wall thickness t of the column hollow square-section and area of the additional longitudinal steel reinforcement in column cross-section A_s with limits from 0 to 1.5 % of concrete area of the column cross-section.

The compression stress-stain curve of the used high-performance fibre reinforced concrete is summarised in Fig. 2.

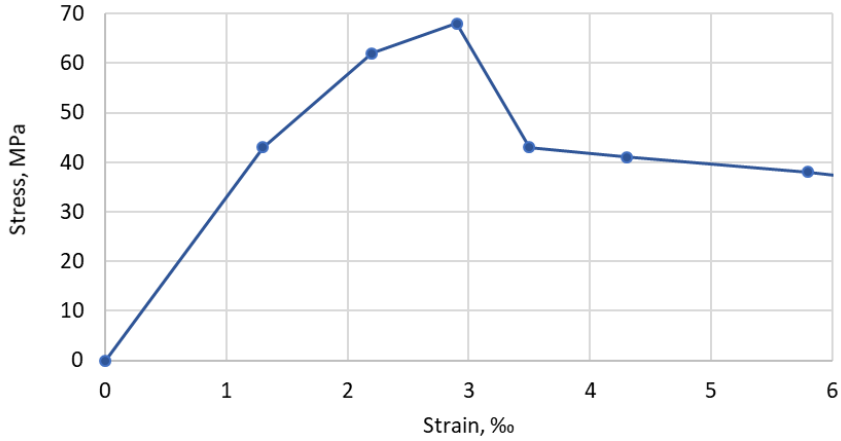

Figure 2. Compression stress-stain curve for high-performance steel fibre concrete.

2.2. Development of analytical simplified ultimate load capacity calculation method

To develop analytical simplified calculation method of column ultimate load capacity for variable column height and material consumption of the steel of the additional longitudinal reinforcement and high-performance concrete, response surface methodology is used. Response surface method is based on the search of adequate polynomial equation, which describes the behaviour of the experimental data set with the objective and makes it possible to predict the results of the objective in some factors interval on which a function was defined.

The dependences of ultimate load capacity of the columns on the height, wall thickness of the hollow square-section and area of the additional longitudinal steel reinforcement in column cross-section as a percentage of the concrete area were obtained as the second-degree polynomial equations. The second-degree polynomial equation is chosen in accordance with the reference's recommendations due to its simplicity and precision [30]. Equation (1) was written for the case, when ultimate load capacity was considered as a parameter of optimization.

$$F,M = b_0 + b_1 H + b_2 t + b_3 A_s + b_{12} Ht + \\ + b_{13} HA_s + b_{23} tA_s + b_{11} H^2 + b_{22} t^2 + b_{33} A_s^2 \quad (1)$$

where: F, M are axial load and bending moment, which characterize ultimate load capacity of the column;

b_i, b_{ij} are coefficients;

H is height of the column, m;

t is wall thickness, cm;

A_s is area of the longitudinal steel reinforcement in column cross-section as a proportion of the concrete area, %.

To receive experimental data set for the prediction of the ultimate load capacity of the column, experimental design with 3 input variables – H, t and A_s with 3 levels of each factor was made. Accepted values for the experiments are shown in Table 1.

Table 1. Experimental design.

Nr.	1	2	3	4	5	6	7	8	9	10	11	12	13	14	15	16	17	18	19	20	21	22	23	24	25	26	27
H, m	3.5	4	4.5	3.5	4	4.5	3.5	4	4.5	3.5	4	4.5	3.5	4	4.5	3.5	4	4.5	3.5	4	4.5	3.5	4	4.5	3.5	4	4.5
t, cm		5			8.5			12			5			8.5			12			5			8.5			12	
A_s, %					0									0.2									1.5				

For all of the 27 experiments calculations are made and ultimate load capacity as a function $F,M = f(H, t, A_s)$ are determined. Relationship between axial force and bending moment value is characterized by equation (2).

$$M = F \cdot e \quad (2)$$

where: M is bending moment acting on the column, kNm;

F is axial load acting on the column, kN;

e is eccentricity, m.

Simplified design scheme of the multi-storey building, where one of the ends of the column is fixed, and loads are transferred from each storey to the column with eccentricity by beams has been adopted, so that the eccentricity of the axial load, which forms a bending moment, is equal to the distance from the centre of the column cross-section to the centre of the hollow square-section wall of the column, according to the Fig. 3.

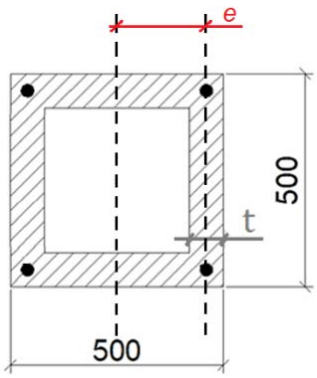

Figure 3. Eccentricity *e* of the column hollow square-section.

The developed 3D and 1D column numerical models, which considered non-linear behaviour of high-performance steel fibre reinforced concrete material by degradation of Young's modulus cause of cracking, are used for the experiment calculations. For the prediction of behaviour of high-performance steel fibre reinforced concrete damage variable is used [3].

Used 3D numerical model is validated by the experimental data from the publication [29] for high-performance steel fibre concrete column with pinned supports at both ends with additional longitudinal reinforcement subjected to compression and flexure, and then, verification of the 1D numerical model of column with fixed support at one end, according to an embodiment, has been done.

2.3. 3D model validation at compressive stress

The developed modelling procedure is validated for high-performance steel fibre reinforced concrete (HPSFRC) column subjected to combined action of compression and bending with additional longitudinal reinforcement. Experimental data from the publication [29] have been used to validate the model.

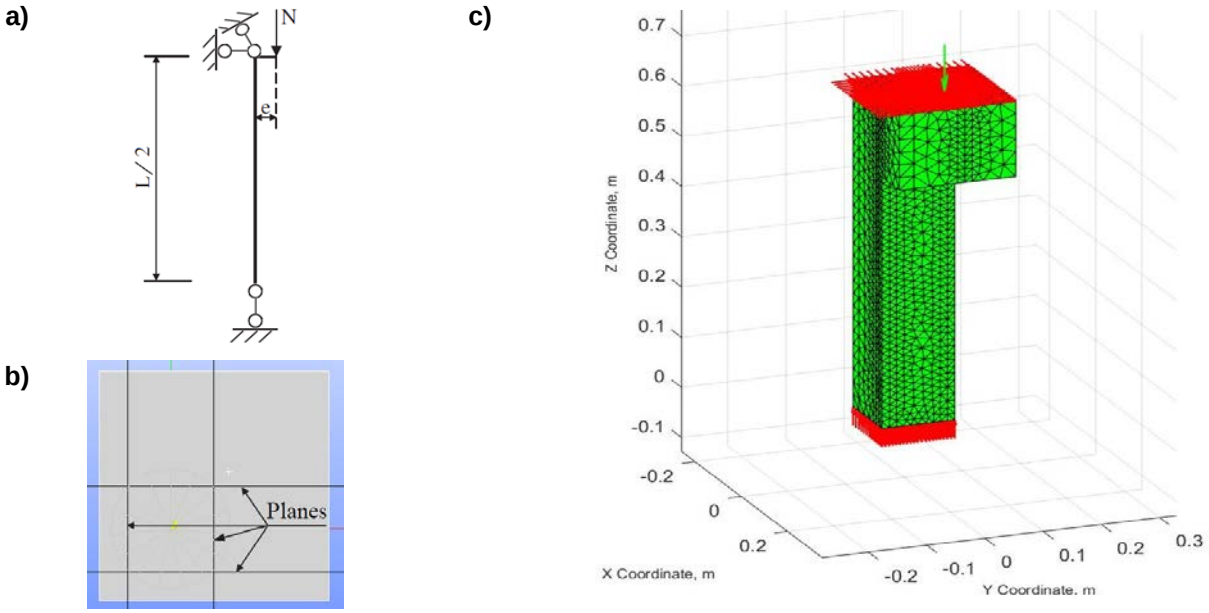

Figure 4. Process of modelling: a) design scheme for calculation of ½ column with *e* = 50 mm and L/2 = 650 mm; b) view from top to column with additional planes for meshing; c) column mesh.

The column 3D model is designed for one-half the length of the column (Fig. 4 a)) to reduce the time of calculation by using symmetry conditions. The model is divided into finite elements in such a way that the volume-type finite elements nodes coincide with the beam-type finite elements nodes, thus ensuring collaboration between concrete and longitudinal reinforcement. For this purpose, additional planes passing through longitudinal bars (Fig. 4 b)) are defined in the modelling process. The meshing of the model in the finite elements is related to these planes (Fig. 4 c)).

2.4. Verification of the 1D numerical model

Calculations with the 3D numerical model are complex and time-consuming, therefore verification of the 1D numerical model of the column with fixed support at one end, which is subjected to the compression and flexure has been done by comparison of the results of calculations with both models.

Calculations of 3 experiments with 3D and 1D model have been made. The values of input variables of these 3 experiments are shown in Table 2.

Table 2. Input variables for 1D model verification.

Nr.	1	2	3
H, m	3.5	4	4.5
t, mm	5	12	8.5
A_s, %	0.2	0	1.5

Verification of the 1D model is made by comparison of either crushing axial load values or load value at displacement value H/250, depending on which value is reached first with calculation results obtained by 3D numerical model. This value of axial load will be called the ultimate load capacity.

3. Results and Discussions

3.1. Accuracy of the 3D model

Based on results of validation, character of the failure scheme for both of 3D numerical model and experimental specimen are similar [31]. Load-displacement curves of column specimen subjected to the compression with flexure, according to laboratory tests and 3D numerical model calculations, are summarized in Fig. 5.

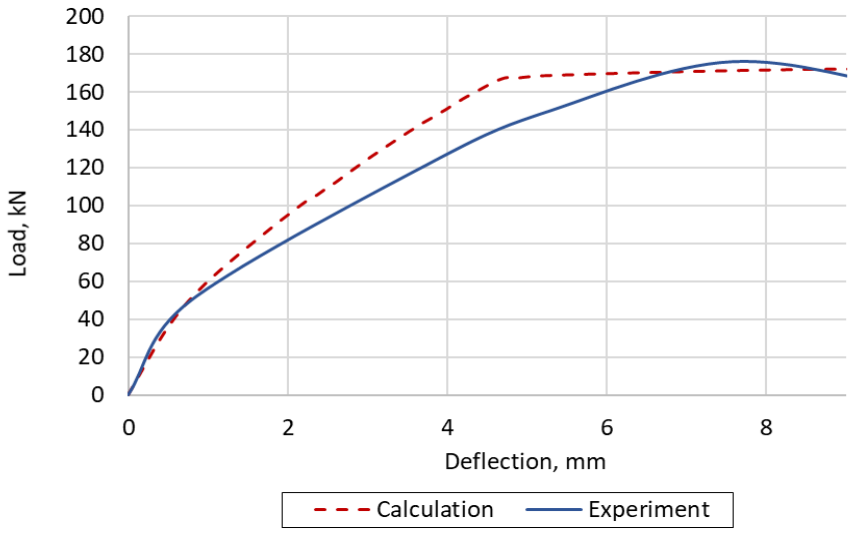

Figure 5. Load-displacement curves for column specimen.

According to the results obtained, the crushing axial load obtained from the laboratory test was 176 kN and bending moment 898.48 kNm, while the calculated by 3D non-linear numerical model crushing axial load was 172.462 kN and corresponding bending moment 862.31 kNm. The difference between design and experimentally determined axial load and bending moment is 2.0 % and 4.0 %, respectively. The behaviour of the calculation model at the linear stage is identical to the actual operation of the column specimen. The plastic behaviour of material is also similar in both cases. The behaviour of the calculation model is like the actual operation of the column specimen and it can be concluded, that developed model is safe for prediction of the behaviour of high-performance steel fibre reinforced concrete material.

3.2. Accuracy of the 1D model

The resulting load-displacement curves of 1D numerical model verification are enclosed in the Fig. 6. According to the results obtained, the load value at displacement value H/250 calculated by 3D and 1D non-linear numerical models for experiment Nr.1 is 353.9 kN and 342 kN, respectively; for experiment Nr.2 is 703.0 kN and 682 kN and for experiment Nr.3 is 823.8 kN and 805 kN. The difference between axial load values determined by 3D and 1D models is between 2.3 % and 3.4 %. As it can be seen from Fig. 6, linear-elastic stage of load-deflection curve obtained by 3D numerical model is until about 96 % of ultimate load capacity of columns, after what plastic stage is started. The 1D model produces more conservative results of the behaviour of the column subjected to the compression and flexure than 3D model. The load-deflection curve obtained by the 1D model is characterized by a more pronounced elastic-plastic stage, especially for specimens with large percentage of additional longitudinal reinforcement.

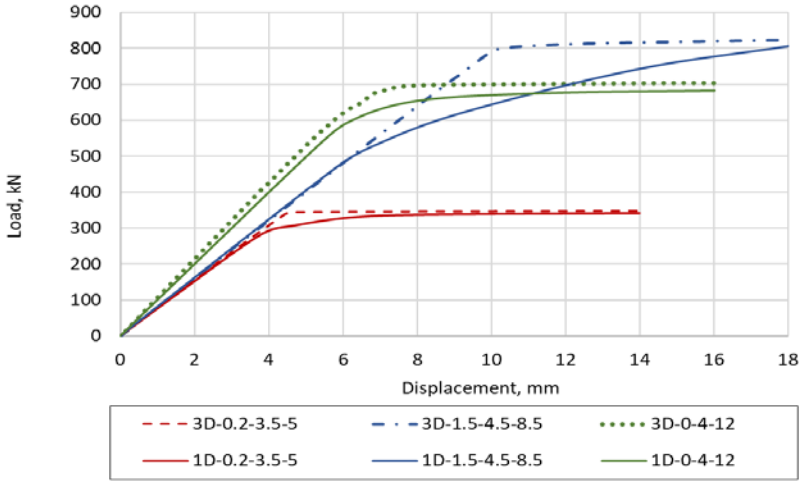

Figure 6. Load-displacement curves for columns, where 3D/1D – results obtained from 3D or 1D model, respectively; -A_s-H-t – values of input variables according Table 2.

The stress and strain profile for typical specimen with input variables 0.2-4-8.5 obtained by 1D model are summarized in Fig. 7. As it can be seen from the Fig. 7, the concrete in the compressed zone still continues to work in the elastic deformation region, while significant plastic deformations develop in the concrete in the tensile zone. The strains in the section are approaching the limiting values that precede the formation of normal cracks in the tensioned zone of the section.

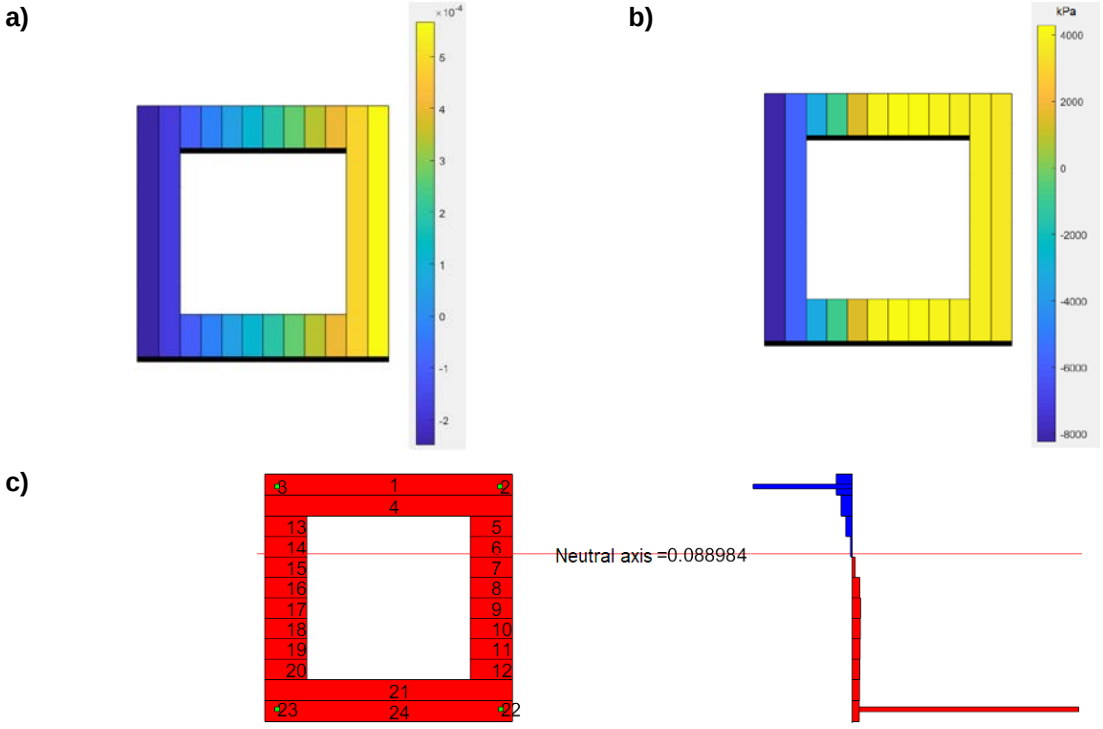

Figure 7. Profiles for specimen with A_s = 0.2 %, H = 4 m, t = 8.5 cm: a) of the strain in concrete material; b) of the stress in concrete material; c) of the stress in all materials of the section.

Taking into account, that the load value at displacement value H / 250 refers to the plastic stage of the load-deflection curve obtained by both of models, 1D model will be used for the further calculations of the experiments.

3.3. Effect of the input variables on the column characteristics

The column height, wall thickness of the hollow square-section and area of the additional longitudinal steel reinforcement in column cross-section as a percentage of the concrete area have different effect on the column characteristics such as ultimate load capacity, column stiffness and energy absorption. The effect of changing the input variables on ultimate load capacity is summarized in the Table 3.

As it can be seen, column height has not large effect on the ultimate load capacity for columns with low percentage of longitudinal reinforcement, only for columns with A_s = 1.5 % ultimate load capacity decreases by 10-11 %.

The biggest effect on the ultimate load capacity leaves a change in the wall thickness of the hollow square-section. For the columns with wall thickness 8.5 and 12 cm the value of ultimate load capacity increases by 59.8-61.9 % and 113-119 %, correspondingly, in comparison with t = 5 cm.

Changes in the amount of reinforcement also have a significant effect. For the column with H = 3.5 m, the ultimate load capacity increases by 6.5-8.4 % and 73.5-78.6 % for the columns with the area of the additional longitudinal steel reinforcement in column cross-section as a percentage of the concrete area 0.2 and 1.5 %, correspondingly, in comparison with column without additional longitudinal reinforcement. But with increasing column height, this effect on ultimate load capacity decreases. At A_s = 1.5 % for columns with height 4 and 4.5 m the effect decreases by 14 and 24 %, correspondingly.

The effect of changing the input variables on column stiffness is summarized in the Fig. 8.

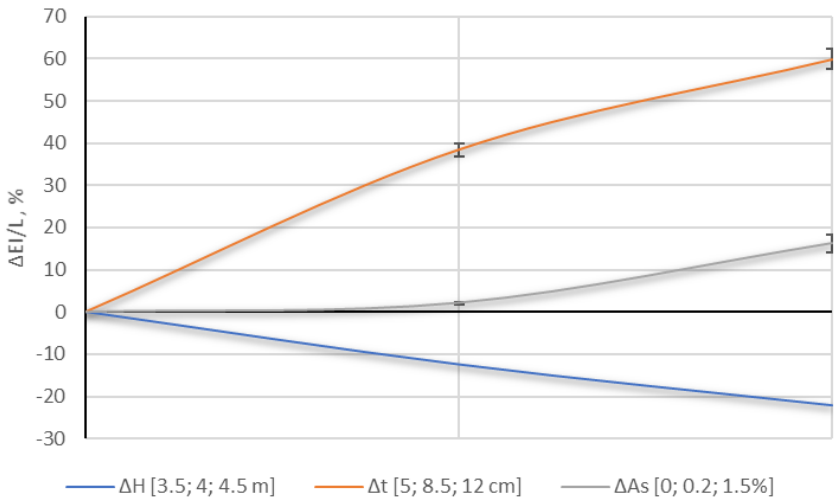

Figure 8. Effect of the changing of input variables H, t and A_s on the column bending stiffness.

As it can be seen from the Fig. 8, the biggest effect on the column bending stiffness, similar as on the ultimate load capacity, leaves a change in the wall thickness of the hollow square-section. For the columns with wall thickness 8.5 and 12 cm the value of bending stiffness increases by 37.2–39.7 % and 57.0–62.7 %, correspondingly, in comparison with t = 5 cm.

Changes in the amount of reinforcement do not have a significant effect on stiffness. For the column with A_s = 0.2 % and A_s = 1.5 %, the bending stiffness increases by 1.9–2.4 % and 14.2–18.3 %, correspondingly, in comparison with columns without additional longitudinal steel reinforcement.

As the height of the column increases, the column bending stiffness decreases. For the columns with height 4 and 4.5 m the value of bending stiffness decreases by 12.5 % and 22.2 %, correspondingly, in comparison with H = 3.5 m.

Table 3. Effect of the input variables on ultimate load capacity.

H, m	3.5	4	4.5	3.5	4	4.5	3.5	4	4.5	3.5	4	4.5	3.5	4	4.5	3.5	4	4.5	3.5	4	4.5	3.5	4	4.5	3.5	4	4.5
t, cm	5			8.5			12			5			8.5			12			5			8.5			12		
A_s, %	0									0.2									1.5								
N_{1D}, kN	321	320	320	513	512	511	683	682	680	342	340	339	550	547	545	740	735	731	557	525	500	902	847	805	1220	1145	1090
ΔH, %	0	-0.3	-0.3	0	-0.2	-0.4	0	-0.1	-0.4	0	-0.6	-0.9	0	-0.5	-0.9	0	-0.7	-1.2	0	-5.7	-10	0	-6.1	-11	0	-6.1	-11

H, m	3.5			4			4.5			3.5			4			4.5			3.5			4			4.5		
t, cm	5	8.5	12	5	8.5	12	5	8.5	12	5	8.5	12	5	8.5	12	5	8.5	12	5	8.5	12	5	8.5	12	5	8.5	12
A_s, %	0									0.2									1.5								
N, kN	321	513	683	320	512	682	320	511	680	342	550	740	340	547	735	339	545	731	557	902	1220	525	847	1145	500	805	1090
Δt, %	0	59.8	113	0	60	113	0	59.7	113	0	60.8	116	0	60.9	116	0	60.8	116	0	61.9	119	0	61.3	118	0	61	118

H, m	3.5									4									4.5								
t, cm	5			8.5			12			5			8.5			12			5			8.5			12		
A_s, %	0	0.2	1.5	0	0.2	1.5	0	0.2	1.5	0	0.2	1.5	0	0.2	1.5	0	0.2	1.5	0	0.2	1.5	0	0.2	1.5	0	0.2	1.5
N, kN	321	342	557	513	550	902	683	740	1220	320	340	525	512	547	847	682	735	1145	320	339	500	511	545	805	680	731	1090
ΔA_s,%	0	6.5	73.5	0	7.2	75.8	0	8.4	78.6	0	6.3	64.1	0	6.8	65.4	0	7.8	67.9	0	5.9	56.3	0	6.7	57.5	0	7.5	60.3

Table 4. Ultimate load capacity of the columns of 27 experiments.

Nr.	1	2	3	4	5	6	7	8	9	10	11	12	13	14	15	16	17	18	19	20	21	22	23	24	25	26	27
H, m	3.5	4	4.5	3.5	4	4.5	3.5	4	4.5	3.5	4	4.5	3.5	4	4.5	3.5	4	4.5	3.5	4	4.5	3.5	4	4.5	3.5	4	4.5
t, cm	5			8.5			12			5			8.5			12			5			8.5			12		
A_s, %	0									0.2									1.5								
N_{1D}, kN	321	320	320	513	512	511	683	682	680	342	340	339	550	547	545	740	735	731	557	525	500	902	847	805	1220	1145	1090
N_{eq}, kN	314	319	329	512	510	514	688	680	677	339	338	342	554	547	544	748	734	724	569	526	488	898	849	804	1207	1150	1099
Δ, %	2.3	0.3	2.9	0.3	0.3	0.5	0.7	0.3	0.5	0.9	0.6	0.8	0.8	0.1	0.2	1.1	0.2	0.9	2.1	0.2	2.3	0.4	0.2	0.1	1.1	0.5	0.8

The effect of changing the input variables on column energy absorption, what is defined as the surface below the load-displacement curve [32], is summarized in the Fig. 9.

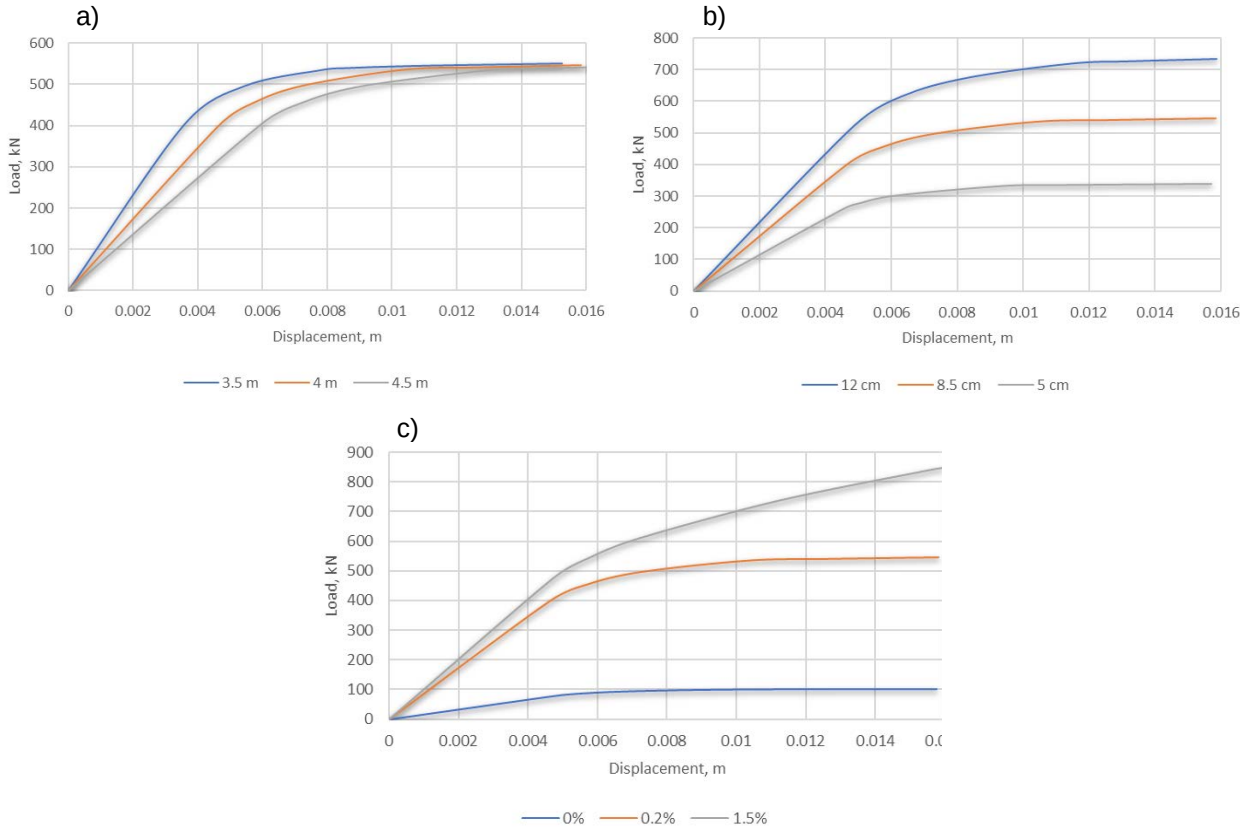

Figure 9. Dependence of the energy absorption for column with H = 4 m, t = 8.5 m and A_s = 0.2 % on changing of a) height, b) wall thickness of the hollow square-section, c) the area of the additional longitudinal steel reinforcement in column cross-section as a percentage of the concrete area.

As it can be seen from the Fig. 9 a) the effect of the column height on the energy absorption is insignificant. The largest increase of energy absorption is observed from the changes in the amount of additional longitudinal reinforcements (Fig. 9 c)). The thickness of the hollow square-section wall has also significant effect. The results obtained coincide with other published researches [33].

3.4. Analytical simplified ultimate load capacity calculation method

Statistic data set of column ultimate load capacity, obtained from calculations of the 27 experiments, makes regression analyses possible. Based on the results of calculations, the coefficients for dependences (3) of ultimate load capacity of the columns on the height, wall thickness of the hollow square-section column and area of the longitudinal steel reinforcement in column cross-section as a percentage of the concrete area were obtained.

$$\begin{aligned} F,M = {} & 21.48 - 41.4 \cdot H + 81.91 \cdot t + \\ & + 218.21 \cdot A_s - 3.86 \cdot Ht - 64.18 \cdot HA_s + \\ & + 25.1 \cdot tA_s + 9.56 \cdot H^2 - 0.88 \cdot t^2 + 33.99 \cdot A_s^2 \end{aligned} \quad (3)$$

where designations are as for equation (1).

The dependence of column ultimate load capacity on material consumption of the steel of the longitudinal reinforcement and high-performance concrete for column with height of 4 m is shown in the Fig. 9.

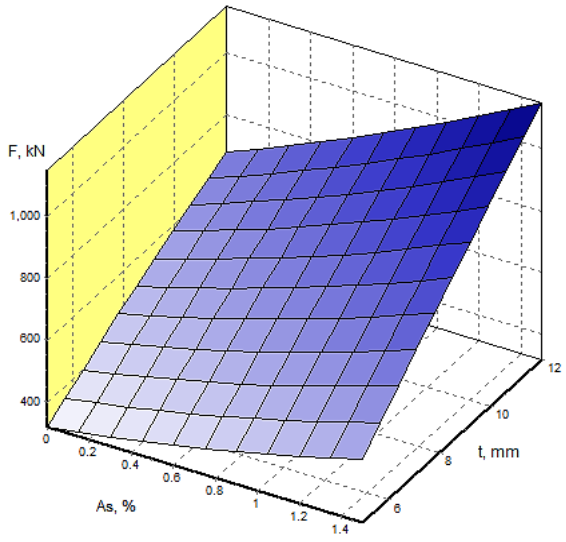

Figure 9. The dependence of column ultimate load capacity (F) on the wall thickness (t) and amount of longitudinal reinforcement (A_s).

The values of ultimate load capacity of the columns of 27 experiments calculated by 1D numerical models (N_{1D}) and by the equation obtained (N_{eq}) and their percentage comparison are summarized in Table 4.

As it can be seen from the Table 4 relative error of ultimate load capacity of the columns predicted by obtained second order polynomial equation (3) for the 27 designed experiments is with limits from 0.1 to 2.9 %.

To check adequacy of the obtained dependence (3) of ultimate load capacity of the columns on the height, wall thickness of the hollow square-section column and area of the additional longitudinal steel reinforcement in column cross-section as a percentage of the concrete area, 3 control calculations for column with random chosen input variables from the region of the interest have been made. The values of input column variables and comparison of obtained results for control calculations are summarized in Table 5.

Table 5. Input variables for control calculations.

Nr.	1	2	3
H, m	3.7	4.1	4.3
t, cm	7	11	6
A_s, %	1.2	0.2	0.7
N_{1D}, kN	676	682	478
N_{eq}, kN	666	681	462
Δ, %	1.5	0.2	3.3

As it can be seen from the results of 3 control calculations (Table 4) relative error of load-bearing capacity predicted by obtained polynomial equation (3) for the 3 control calculations is from 0.2 to 3.3 %, so the obtained by regression analyses equation fits well the ultimate load capacity of the 1D numerical model of the column subjected to the compression and flexure, therefore the use of the equation (3) as analytical simplified column load-bearing capacity calculation method is justified.

4. Conclusions

Numerical models of high-performance steel fibre reinforced concrete columns were checked and showed adequate results. Analytical simplified calculation method that approximate output results of finite elements calculations for high-performance steel fibre reinforced concrete columns subjected to the compression and flexure with complicate hollow square-section was developed. The obtained second-degree polynomial equation makes it possible to predict the results of the ultimate load capacity of the column in selected the factors interval on which a function was defined with sufficient precision.

The results showed that:

- 3D numerical model fits the behaviour of compression elements and makes it possible to determine ultimate load of column with about 98 % precision;
- The using of 1D numerical model provides more conservative result than 3D numerical model, the difference of determined ultimate load capacity is up to 3.4 %, but 1D model can significantly reduce the time required for calculations;
- The wall thickness of the hollow square-section and area of the additional longitudinal steel reinforcement in column cross-section as a percentage of the concrete area have significant effect on the column characteristics such as ultimate load capacity, column bending stiffness and energy absorption, at the time when changes of the column height have negligible impact on the column characteristics;
- Obtained equation for prediction of ultimate load capacity of the column with random chosen parameters of cross-section from the factors interval on which a function was defined allows to determine it with precision more than 96 %.

5. Acknowledgements

Financial support: European Regional Development Fund project Nr.1.1.1.1/16/A/007 “A New Concept for Sustainable and Nearly Zero-Energy Buildings”.

References

1. Vougioukas, E., Papadatou, M. A model for the prediction of the tensile strength of fiber-reinforced concrete members, before and after cracking. Fibers. 2017. Vol. 5. No. 3. Article No. 27.
2. Olivito, R.S., Zuccarello, F.A. An experimental study on the tensile strength of steel fiber reinforced concrete. Composites: Part B. 2010. Vol. 41. Pp. 246–255.
3. Buka-Vaivade, K., Sliseris, J., Serdjuks, D., Pakrastins, L., Vatin, N.I. Rational use of HPSFRC in multi-storey building. Magazine of Civil Engineering. 2018. Vol. 84. No. 8. Pp. 3–14.
4. Klyuev S.V., Klyuev A.V., Abakarov A.D., Shorstova E.S., Gafarova N.G. The effect of particulate reinforcement on strength and deformation characteristics of fine-grained concrete. Magazine of Civil Engineering. 2017. Vol. 75. No. 7. Pp. 66–75.
5. Singh, H. Steel fiber reinforced concrete – behavior, modelling and design. Ludhiana: Springer, 2017, 172 p.
6. Kazemi, M.T., Golsorkhtabar, H., Beygi, M.H.A., Gholamitabar, M. Fracture properties of steel fiber reinforced high strength concrete using work of fracture and size effect methods. Construction and Building Materials. 2017. Vol. 142. Pp. 482–489.
7. Ulas, M.A., Alyamac, K.E., Ulucan, Z.C. Effects of aggregate grading on the properties of steel fibre-reinforced concrete. IOP Conference Series: Materials Science and Engineering. 9th International Conference Fibre Concrete 2017, Prague, Czech Republic, September 13-16, 2017. Vol. 246, No. 1. Article No. 012015.
8. Nikolenko, S.D., Sushko, E.A., Sazonova, S.A., Odnolko, A.A., Manokhin, V.Ya. Behaviour of concrete with a disperse reinforcement under dynamic loads. Magazine of Civil Engineering. 2017. No. 7. Pp. 3–14.
9. Simões, T., Octávio, C., Valença, J., Costa, H., Dias-da-Costa, D., Júlio, E. Influence of concrete strength and steel fibre geometry on the fibre/matrix interface. Composites Part B: Engineering. 2017. Vol. 122. Pp. 156–164.
10. Balanji, E. K. Z., Sheikh, M.N., Hadi, M.N.S. Behavior of hybrid steel fiber reinforced high strength concrete. Proceedings of the First European and Mediterranean Structural Engineering and Construction Conference EURO-MED-SEC-1, Istanbul, Turkey, May 24-29, 2016. Pp. 29–34.
11. Travush, V.I., Konin, D.V., Krylov, A.S. Strength of reinforced concrete beams of high-performance concrete and fiber reinforced concrete. Magazine of Civil Engineering. 2018. No. 1. Pp. 90–100.
12. Savita, Shwetha S., Malanbi, Shweta, Saksheshwari, Manjunath K. Experimental study on strength parameters of steel fiber reinforced concrete using GI wire & fly ash. International Research Journal of Engineering and Technology. 2018. Vol. 5. No. 5. Pp. 3271–3277.
13. Kirsanov, A.I., Stolyarov, O.N. Mechanical properties of synthetic fibers applied to concrete reinforcement. Magazine of Civil Engineering. 2018. Vol. 80. No. 4. Pp. 15–23.
14. Taheri Fard, A.R., Soheili, H., Ramzani Movafagh, S., Farnood Ahmadi, P. Combined effect of glass fiber and polypropylene fiber on mechanical properties of self-compacting concrete. Magazine of Civil Engineering. 2016. Vol. 62. No. 2. Pp. 26–31.
15. Lignola, G.P., Prota, A., Manfredi, G., Cosenza E. Modeling of RC hollow square columns wrapped with CFRP under shear-type load. 2008. Proceedings of the 4th International Conference on FRP Composites in Civil Engineering, CICE 2008.
16. Liang, X., Sritharan, S. Effects of confinement in square hollow concrete column sections. Engineering Structures. 2019. Vol. 191. Pp. 526–535.
17. Abbass, A.A., Abid, S.R., Arna'ot, F.H., Al-Ameri, R.A., Ozakca, M. Flexural response of hollow high strength concrete beams considering different size reductions. Structures. 2020. Vol. 23. Pp. 69–86.
18. Al-Gasham, T.S., Mhalhal, J.M., Jabir, H.A. Influence of post-heating on the behavior of reinforced self-compacting concrete hollow columns. Structures. 2019. Vol. 22. Pp. 266–277.
19. AlAjarmeh, O.S., Manalo, A.C., Benmokrane, B., Karunasena, K., Ferdous, W., Mendis, P. Hollow concrete columns: Review of structural behavior and new designs using GFRP reinforcement. Engineering Structures. 2020. Vol. 203. 109829.
20. Cassese, P., Ricci, P., Verderame, G.M. Experimental study on the seismic performance of existing reinforced concrete bridge piers with hollow rectangular section. Engineering Structures. 2017. Vol. 144. Pp. 88–106.
21. Azzawi, R., Abolmaail, A. Experimental investigation of steel fiber RC hollow columns under eccentric loading. Structures. 2020. Vol. 24. Pp. 456–463.
22. Arani, K.S., Zandi, Y., Pham, B.T., Mu'azu, M.A., Katebi, J., Mohammadhassani, M., Khalafi, S., Mohamad, E.T., Wakil, K., Khorami, M. Computational optimized finite element modelling of mechanical interaction of concrete with fiber reinforced polymer. Computers and Concrete. 2019. Vol. 23. No. 1. Pp. 61–68.

23. Tysmans, T., Wozniak, M., Remy, O., Vantomme, J. Finite element modelling of the biaxial behaviour of high-performance fibre-reinforced cement composites (HPFRCC) using Concrete Damaged Plasticity. Finite Elements in Analysis and Design. 2015. Vol. 100. Pp. 47–53.
24. Hameed, R., Sellier, A., Turatsinze, A., Duprat, F. Metallic fiber-reinforced concrete behaviour: Experiments and constitutive law for finite element modeling. Engineering Fracture Mechanics. 2013. Vol. 103. Pp. 124–131.
25. Ibrahim, A.M., Mahmood, M.S. Finite element modeling of reinforced concrete beams strengthened with FRP laminates. European Journal of Scientific Research. 2009. Vol. 30. No. 4. Pp. 526–541.
26. Buljak, V., Oesch, T., Bruno, G. Simulating fiber-reinforced concrete mechanical performance using CT-based fiber orientation data. Materials (Basel). 2019. Vol. 12. No. 5. 717.
27. Buka-Vaivade, K., Sliseris, J., Serdjuks, D., Sahmenko, G., Pakrastins, L. Numerical Comparison of HPFRC and HPC Ribbed Slabs. IOP Conference Series: Materials Science and Engineering. 2019. Vol. 660. 012054.
28. EN 1992-1-1: Eurocode 2: Design of concrete structures – Part 1-1: General rules and rules for buildings.
29. Tokgoz, S., Dundar, C., Tanrikulu, A. K. Experimental behavior of steel fiber high strength reinforced concrete and composite columns. Journal of Constructional Steel Research. 2012. Vol. 74. Pp. 98–107.
30. Saknite, T., Serdjuks, D., Goremikins, V., Pakrastins, L., Vatin, N.I. Fire design of arch-type timber roof. Magazine of Civil Engineering. 2016. Vol. 64. No. 4. Pp. 26–39.
31. Sliseris, J., Buka-Vaivade, K. Numerical Modelling of High Strength Fibre-Concrete's columns in Multi-Storey Building. IOP Conference Series: Materials Science and Engineering. 2019. Vol. 660. 012062.
32. Nurul Fazita, M.R., Abdul Khalil, H.P.S., Nor Amira Izzati, A., Rizal, S. Effects of strain rate on failure mechanisms and energy absorption in polymer composites. Failure Analysis in Biocomposites, Fibre-Reinforced Composites and Hybrid Composites. 2018. Pp. 51–78.
33. Kim, C.S., Hwang, H.J. Numerical Investigation on Load-carrying Capacity of HSC Encased Steel Angle Columns. Int. J. Concr. Struct. Mater. 2018. Vol. 12. 11.

Contacts:

Karina Buka-Vaivade, karina.buka.vaivade@gmail.com
Dmitrijs Serdjuks, Dmitrijs.Serdjuks@rtu.lv
Janis Sliseris, janis.sliseris@rtu.lv
Leonids Pakrastins, leonids.pakrastins@rtu.lv
Nikolai Vatin, vatin@mail.ru